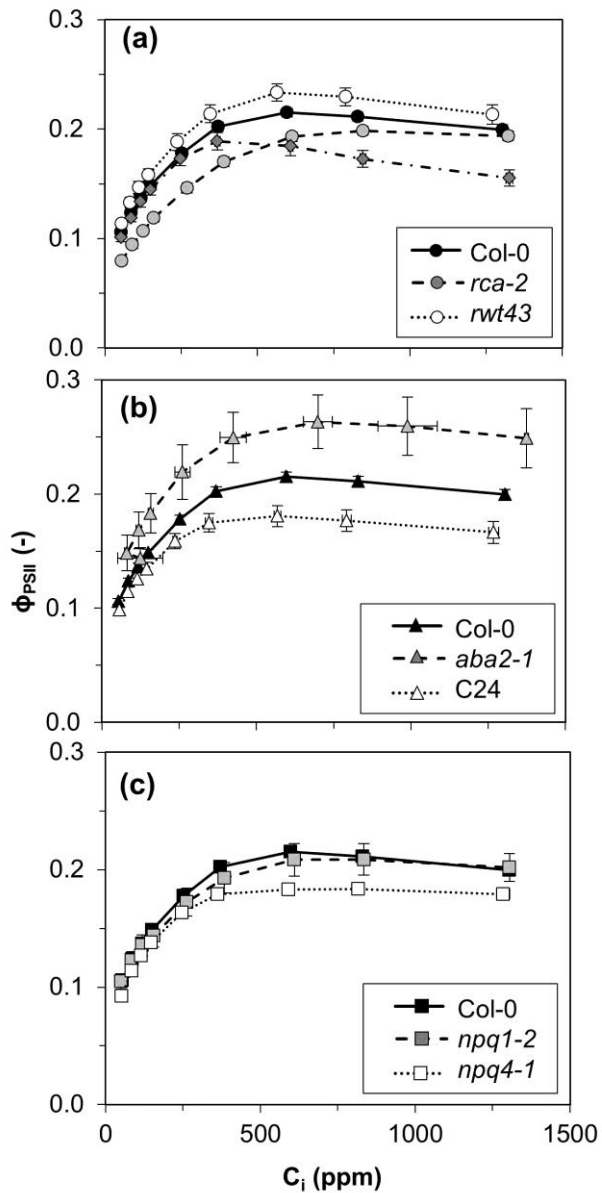


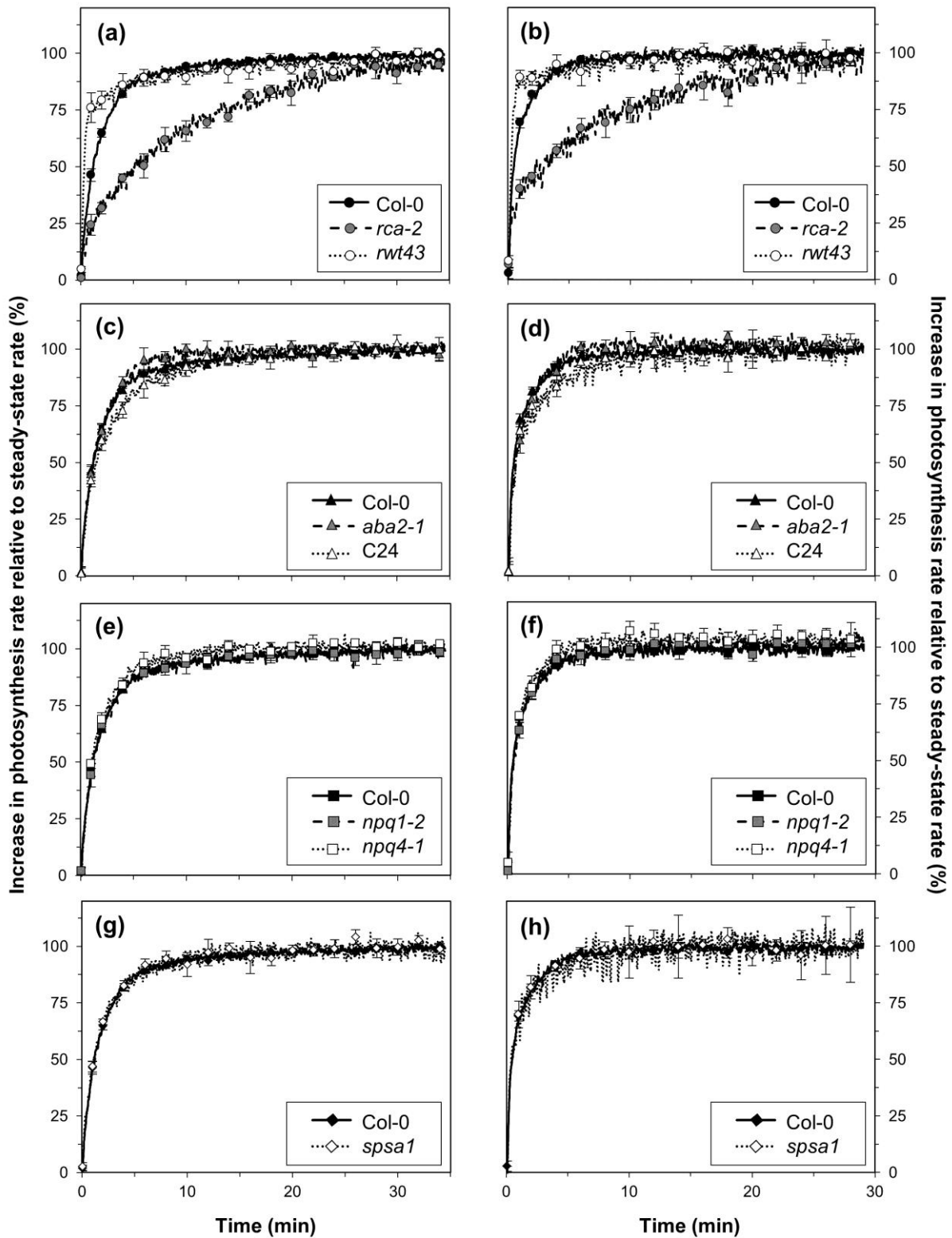
Supplementary material

Metabolic and diffusional limitations of photosynthesis in fluctuating irradiance in *Arabidopsis thaliana*

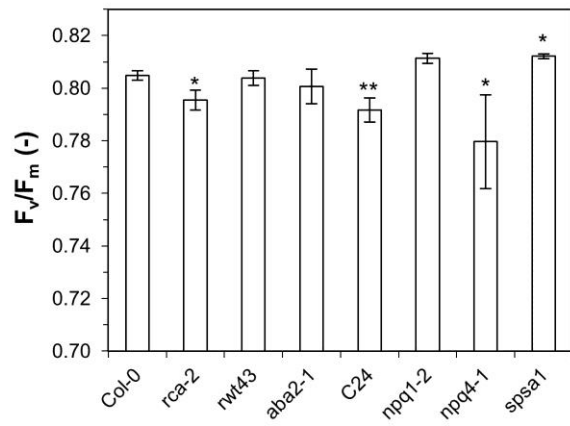
Elias Kaiser, Alejandro Morales, Jeremy Harbinson, Ep Heuvelink, Aina E. Prinzenberg & Leo F.M. Marcelis



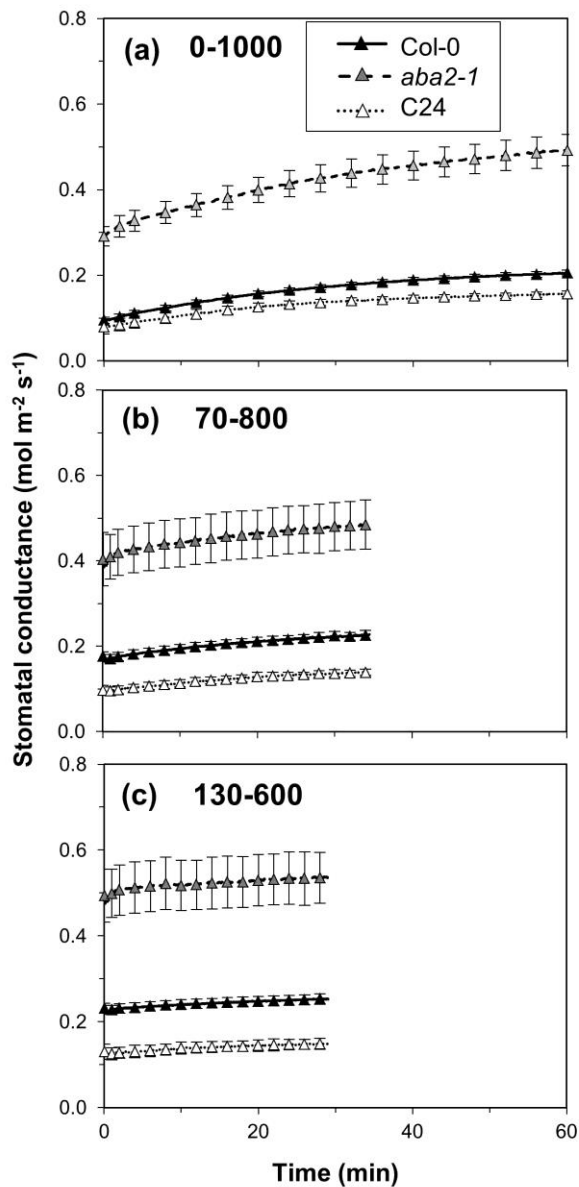
Supplementary Fig. 1. CO₂ response of ϕ_{PSII} in *Arabidopsis* genotypes. Averages \pm SEM, n = 5-15



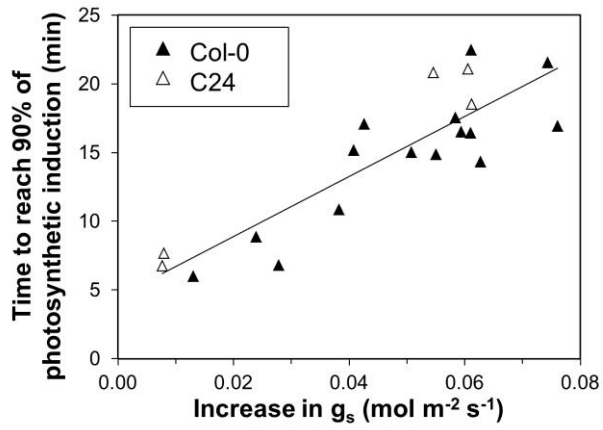
Supplementary Fig. 2. Relative responses of net photosynthesis rates to increases in irradiance, from 70 to 800 (left panel: a, c, e, g) and from 130 to 600 $\mu\text{mol m}^{-2} \text{s}^{-1}$ (right panel: b, d, f, h). Averages \pm SEM, $n = 5-15$



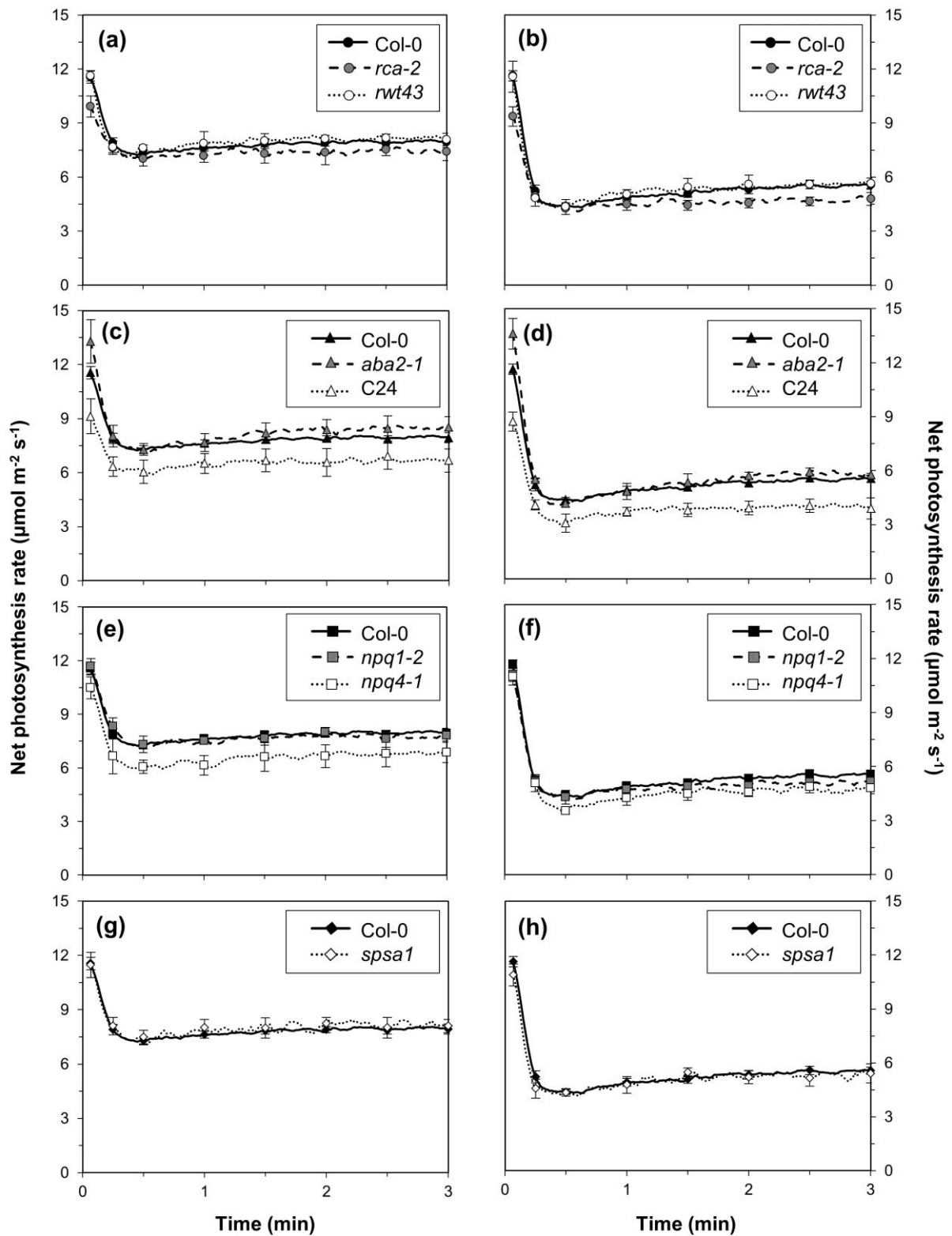
Supplementary Fig. 3. Dark-adapted F_v/F_m in Arabidopsis genotypes after 60 minutes of dark adaptation. Stars denote significant difference from Col-0, as $P < 0.05$ (*) and $P < 0.01$ (**). Averages \pm SEM, $n = 5-15$



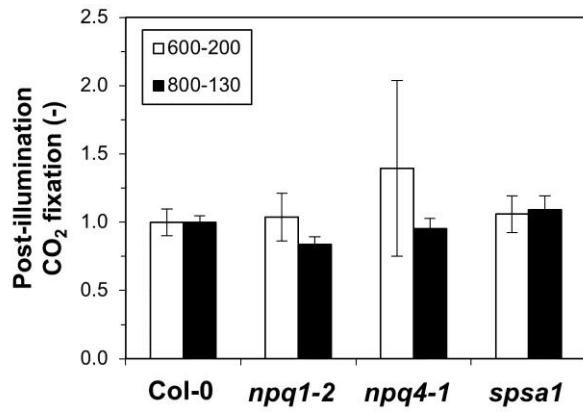
Supplementary Fig. 4. Increases in stomatal conductance in Col-0, *aba2-1* and C24 after step increases in irradiance, a) 0→1000, b) 70→800 and c) 130→600 $\mu\text{mol m}^{-2} \text{s}^{-1}$. Averages \pm SEM, $n = 5-15$



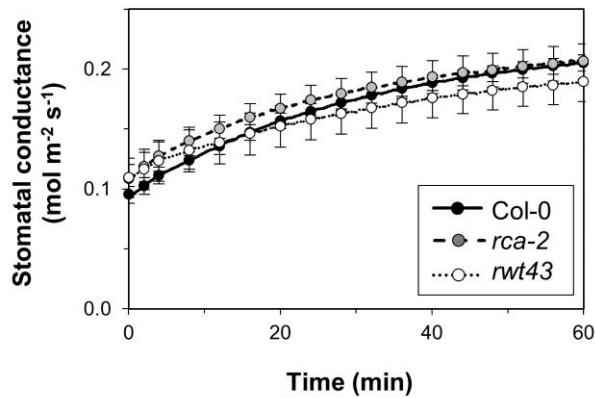
Supplementary Fig. 5. Relationship between the increase in g_s and the time to reach 90% of final photosynthesis rates after a step increase in irradiance (0-1000 $\mu\text{mol m}^{-2} \text{s}^{-1}$) in single replicates of Col-0 and C24 ($R^2 = 0.75$)



Supplementary Fig. 6. Responses of net photosynthesis rates to step decreases in irradiance, from 600 to 200 (left panel: a, c, e, g) and from 800 to 130 $\mu\text{mol m}^{-2} \text{s}^{-1}$ (right panel: b, d, f, h). Averages \pm SEM, $n = 5-15$



Supplementary Fig. 7. Relative post-illumination CO_2 fixation in Col-0, *npq1-2*, *npq4-1* and *spsa1*. Values are expressed relative to Col-0, which was $52 \pm 5 \mu\text{mol m}^{-2}$ after $600 \rightarrow 200 \mu\text{mol m}^{-2} \text{s}^{-1}$ step decreases (white bars) and $76 \pm 3 \mu\text{mol m}^{-2}$ after $800 \rightarrow 130 \mu\text{mol m}^{-2} \text{s}^{-1}$ step decreases (black bars). Averages \pm SEM, $n = 5-15$



Supplementary Fig. 8. Increases in stomatal conductance in genotypes differing in Rubisco activation rate after a $0-1000 \mu\text{mol m}^{-2} \text{s}^{-1}$ step increase

Supplementary Text 1: Calculation of Rubisco activase content

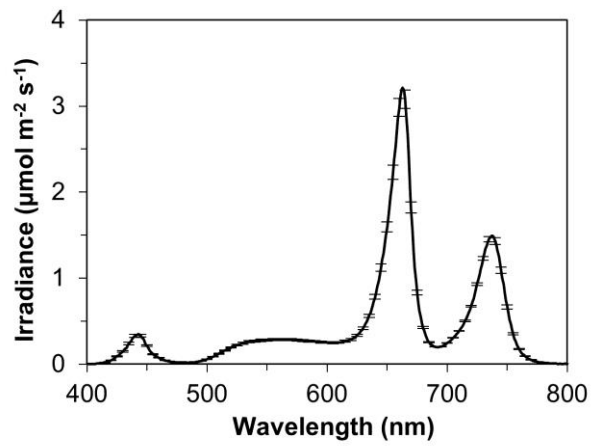
Mott and Woodrow¹ calculated the maximum fraction of Rubisco activation (f_{RB} , achieved at ambient CO₂ concentration and saturating irradiance) from the amount of RCA (mg m⁻²) in a non-linear manner as follows:

$$f_{RB} = \frac{RCA}{RCA + K_A^{RCA}}, \quad (S1)$$

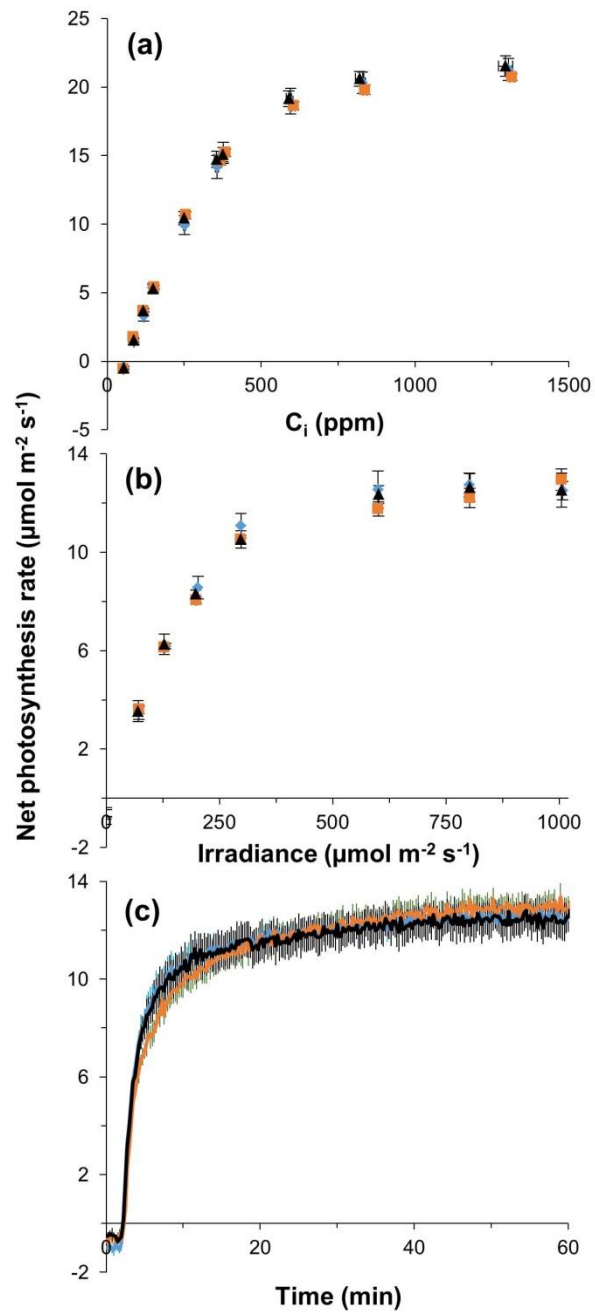
where K_A^{RCA} (mg m⁻²) is the amount of Rubisco activase at which half of the maximum fraction of Rubisco activation is achieved. Carmo-Silva and Salvucci² reported, for leaves of *A. thaliana* Col-0, grown at similar conditions to the plants in our experiments, a maximum fraction of Rubisco activation of 0.91 (i.e. Rubisco is never fully activated). With the value of $K_A^{RCA} = 12.3$ mg m⁻² reported by Mott and Woodrow¹ we can derive that the amount of Rubisco activase in Col-0 is 124.4 mg m⁻². Assuming that the total amount of Rubisco in Col-0 and *rca-2* is the same, we deduce the amount of Rubisco activase using Equation S1 and our values of V_{cmax} in Col-0 (53 ± 1 $\mu\text{mol m}^{-2} \text{s}^{-1}$) and *rca-2* (40 ± 1 $\mu\text{mol m}^{-2} \text{s}^{-1}$), which results in a value of 27 mg m⁻², that is, 22% of the wildtype level.

References

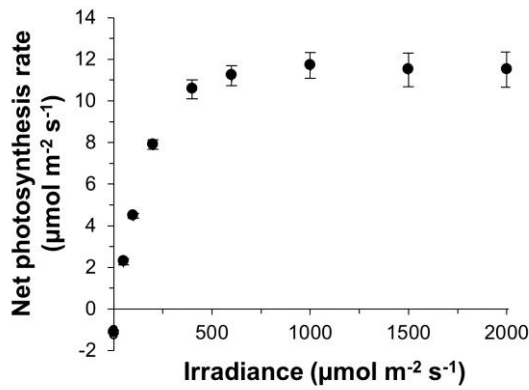
- 1 Mott, K. A. & Woodrow, I. E. Modelling the role of Rubisco activase in limiting non-steady-state photosynthesis. *Journal of Experimental Botany* **51**, 399-406 (2000).
- 2 Carmo-Silva, A. E. & Salvucci, M. E. The regulatory properties of Rubisco activase differ among species and affect photosynthetic induction during light transitions. *Plant Physiology* **161**, 1645-1655, doi:10.1104/pp.112.213348 (2013).



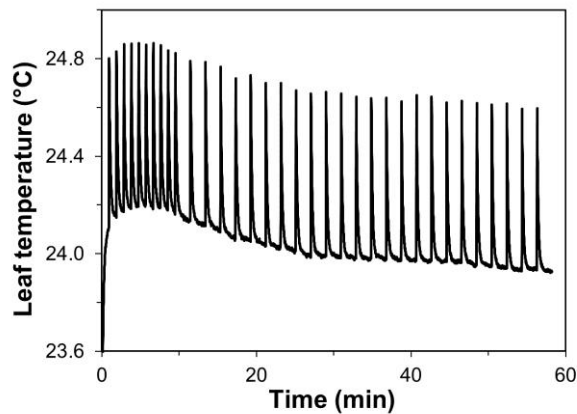
Supplementary Fig. 9. Irradiance spectrum in the growth chamber. Average \pm SEM, $n = 4$



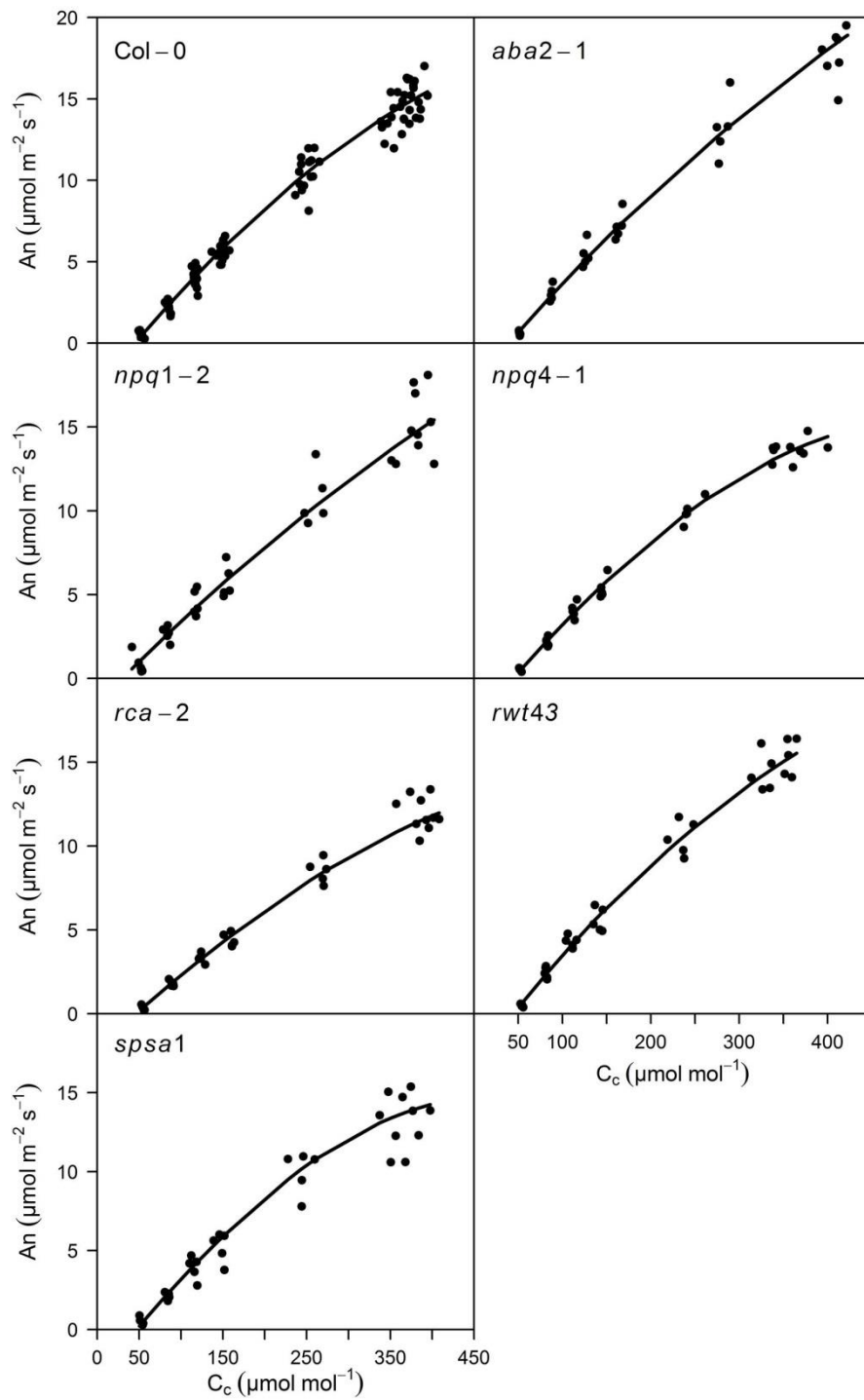
Supplementary Fig. 10. CO₂ response (a), irradiance response (b) and photosynthetic induction (c) in three batches of Col-0, grown sequentially in the same growth system. Batch 1, blue symbols; batch 2, orange symbols; batch 3, black symbols. Average \pm SEM, n = 5



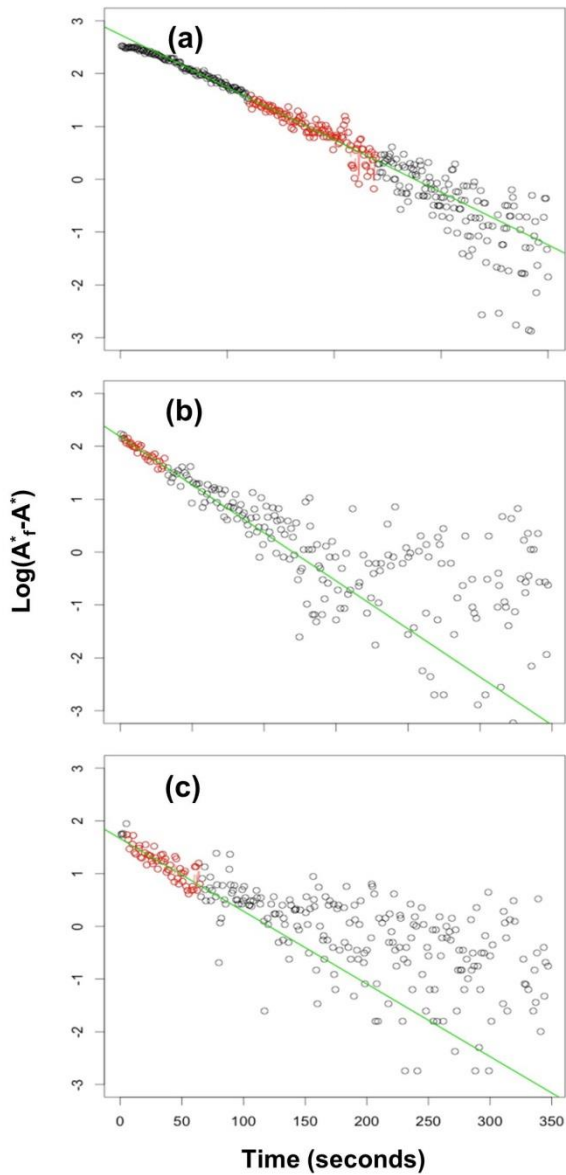
Supplementary Fig. 11. Irradiance response curves of net photosynthesis rate determined on leaves of Col-0 prior to starting the main experiment. These data were used to determine the irradiance levels to be used during for stepwise increases and decreases in irradiance



Supplementary Fig. 12. Time course of leaf temperature on a leaf of Col-0 after a stepwise increase from 0 to 1000 $\mu\text{mol m}^{-2} \text{s}^{-1}$. The spikes in leaf temperature are the results of the regular application of saturating flashes used to determine F_m' , and are representative of all genotypes tested



Supplementary Fig. 13. Local polynomial regression fits through data depicting the steady-state A_n/C_c response. The fits were used for correcting the effects of changes in C_i during photosynthetic induction



Supplementary Fig. 14. Example of data used to calculate the apparent time constant of Rubisco activation (τ_R) after step increases in irradiance a) 0→1000, b) 70→800 and c) 130→600 $\mu\text{mol m}^{-2} \text{s}^{-1}$. Red dots indicate the data points used to calculate τ_R , which is equal to the inverse of the slope of the green line. Explanation of abbreviations on Y-axis: log, natural logarithm; A_f , steady-state net photosynthesis rate at full photosynthetic induction; A^* , transient net photosynthesis rate after irradiance increase, corrected for changes in C_i